Chance and pleiotropy dominate genetic diversity in complex bacterial environments

Lianet Noda-Garcia[1], Dan Davidi[2], Elisa Korenblum[2], Assaf Elazar[1], Ekaterina Putintseva[3], Asaph Aharoni[2] & Dan S. Tawfik[1,*]

[1]Department of Biomolecular Sciences, Weizmann Institute of Science, Rehovot 76100, Israel.

[2]Department of Plant and Environmental Sciences, Weizmann Institute of Science, Rehovot 76100, Israel.

[3]Institutes of Science and Technology, Klosterneuburg, Austria.

* Corresponding author; e-mail: dan.tawfik@weizmann.ac.il.

Abstract

How does environmental complexity affect the evolution of single genes? Here, we measured the effects of a set of mutants of *Bacillus subtilis* glutamate dehydrogenase across 19 different environments – from homogenous single cell populations in liquid media to heterogeneous biofilms, plant roots and soil communities. The effects of individual gene mutations on organismal fitness were highly reproducible in liquid cultures. Strikingly, however, 84% of the tested alleles showed opposing fitness effects under different growth conditions (environmental pleiotropy). In biofilms and soil samples, different alleles dominated in parallel replica experiments. Accordingly, we found that in these heterogeneous cell communities the fate of mutations was dictated by a combination of selection and drift. The latter relates to programmed prophage excisions that occurred along biofilm development. Overall, per individual condition, by the combined action of selection, pleiotropy and chance, a wide range of glutamate dehydrogenase mutations persisted and sometimes fixated. However, across longer periods and multiple environments, nearly all this diversity would be lost – indeed, considering all environments and conditions we have tested, wild-type is the fittest allele.

38 The function of most genes may be essential in some conditions, but only
39 marginally contributing or even deleterious in other conditions [1–4]. The effects of
40 mutations on organismal fitness are therefore environment-dependent, giving
41 rise to complex, pleiotropic genotype-by-environment interactions [5,6]. (Here, we
42 refer to different effects of the same mutation as 'environmental pleiotropy' [7], or
43 'pleiotropy' for brevity, and opposing effects in different environments as
44 'antagonistic pleiotropy'). Moreover, bacterial populations often do not comprise
45 single cells, but rather have a structure as in biofilms. Under this complexity:
46 changing environments and heterogeneous communities (cell or/and species
47 wise), the fate of mutations could also be dictated by population bottlenecks
48 (drift) or rapid takeover of beneficial mutations in other genes (selective
49 sweeps) [8–10]. Consequently, the frequency of a given gene allele may change
50 dramatically (from perishing to fixation) with no relation to its protein function
51 [11,12].

52 We aimed at an experimental setup that would examine how complex
53 bacterial growth states and environments might shape protein evolution.
54 Previous systematic mappings were based on a direct linkage between protein
55 stability and function and organismal survival, thus enabling measurements of
56 effects of mutations at the protein level [5,13–16]. However, how mutations in a
57 single gene-protein affect organismal fitness under varying environments and
58 conditions is largely unexplored [17]. We thus chose as our model *Bacillus subtilis*
59 NCIB 3610, a non-domesticated strain capable of growing in diverse aquatic and
60 terrestrial environments [18]. We explored the effects of mutations in different
61 conditions: in dispersed cells in liquid, but also in biofilms where phenotypic and
62 genetic variability prevails [12]. We also mapped the effects of mutations during

63 spore formation and germination [19] and in more complex and close to natural
64 environments including soil, rhizosphere and plant roots.

65 A catabolic glutamate dehydrogenase (GDH) was our model protein. This
66 enzyme is essential when amino acids such as proline serve as sole carbon-
67 nitrogen sources [20]. However, in the presence of ammonia and glycolytic sugars,
68 GDH activity is redundant as glutamate must be synthesized rather than
69 catabolized. GDHs therefore respond to changes in carbon-nitrogen sources, and
70 as regulators of glutamate homeostasis, are also associated with biofilm
71 development [21,22]. *B. subtilis* has two catabolic GDHs, RocG and GudB. The latter
72 is constitutively expressed, and is regulated via association of its hexameric form
73 [23]. GudB has also regulatory roles [24,25] via interactions with the transcriptional
74 activator of glutamate synthase [25] and with a transcription termination factor
75 that modulates the stringent response [26]. We explored mutations in the
76 oligomeric interface of GudB, aiming at multilateral effects on GudB's enzymatic
77 and regulatory functions.

78 Altogether, these choices of organism and enzyme allowed us to readily
79 examine and quantify the fate of GudB alleles in a range of different growth
80 conditions and environments, also mimicking natural habitats where strong
81 evolutionary forces act [12].

82

83 **Experimental setup and data processing**

84 We anticipated that the effects of the explored mutations would be complex and
85 condition-dependent. We thus opted for deep rather than broad coverage and
86 mapped 10 positions within a single ~150 base pairs segment that resides at
87 GudB's oligomeric interface. The mutagenized positions were arbitrarily chosen

88 while aiming to map highly conserved positions (*e.g.* 58, D in all GudB
89 orthologues) as well as diverged ones (*e.g.* 48, or 61; variable amongst GudB
90 orthologues; **Table S1**). The mutagenized codons were diversified to NNS,
91 whereby N represents any of the 4 bases, and S represents G or C. We thus
92 created 10 libraries, each diversifying a single position into 20 different amino
93 acids *plus* a stop-codon. The libraries were incorporated into the chromosome of
94 *B. subtilis* NCIB 3610 under *gudB*'s original promoter and terminator. The
95 combined library contained 320 single mutant alleles, whose genomes differ, in
96 principle, by a single GudB mutation, including 200 different amino acid alleles
97 (including wild-type), 10 stop-codons, and also synonymous alleles whereby the
98 same amino acid could be encoded by 2 or 3 different codons.

99 This starting library (the initial mix, hereafter) was used to inoculate
100 cultures grown in an array of different conditions. We tested 7 different growth
101 states with diverse complexity, from single cells to communities: liquid, pellicles
102 (air-liquid biofilms), spores, germinated spores, biofilms grown on agar
103 including on carbon-nitrogen gradients, and colonized soil. Up to 5 different
104 carbon-nitrogen sources were used that, at least as far as the phenotypes of the
105 GudB knockout indicate, inflict different levels of selection on GudB: Glutamate
106 *plus* ammonia (GA) where ΔGudB has no growth effect; glutamate *plus* glycerol
107 (GG), arginine (A), and arginine *plus* proline (PA), where ΔGudB exhibits a slight
108 growth defect, and proline (P) where ΔGudB exhibits the strongest growth defect
109 (**Fig. S1**). In total, we tested 19 conditions. At each condition, three to five
110 biological replicas were performed by inoculating from the same initial mix. The
111 replicas were grown in parallel, and individually analyzed. Illumina sequencing
112 was applied to determine the frequency of each of the *gudB* alleles in the initial

113 mix and after growth. Following filtering (see Methods), we obtained data for
114 244 up to 269 individual alleles per experiment (**Data S1** & **Fig. S2).**
115 The ratio between an allele's frequency at the end of growth and in the
116 initial mix was derived, and this ratio is referred to as the frequency coefficient
117 (FC; **Data S2**). Basically, FC > 1 means an enriched, beneficial mutation, and FC <
118 1 a purged deleterious one. However, given the experimental error in
119 determining FC values, values between 0.8 and 1.2 were classified as 'neutral', FC
120 ≤0.8 assigned a mutation as 'deleterious', and FC >1.2 as 'beneficial' (see
121 Methods). Mutations with FC ≤0.1 were classified as 'highly deleterious', and
122 similarly, FC ≥10 as 'highly beneficial'. FC values reflect the relative frequency of
123 alleles, and therefore relate logarithmically to their relative fitness effects (or
124 selection coefficient, *s*). Hence, logFC values were compared throughout. Note,
125 however, that the number of generations differs fundamentally between
126 conditions – *e.g.* ~50 generations in liquid (following 5 serial transfers into a
127 fresh culture) versus effectively no replication in spores (a dormant non-
128 replicative form of *B. subtilis*). Moreover, in pellicles and biofilms, the number of
129 generations cannot be easily determined, and in biofilms different cell types (*i.e.*
130 matrix producers, dormant cells, etc.) have different growth rates [27,28]. So, while
131 we could not calculate selection coefficients, one should keep in mind that an FC
132 value of 0.8 in spores would effectively mean extinction across 50 generations in
133 liquid ($0.8^{50} = 10^{-5}$).
134

135 **Irreproducibility – selection *versus* drift**

136 Our first observations indicated two contrasting scenarios. In liquid cultures, for
137 example, we observed highly reproducible FC values between biological replicas

138 (**Fig. 1a**). Given the small sample numbers (3 replicas as standard, 5 in few
139 cases) the observed variance may underestimate the actual variance. However,
140 the repetitively low variance in a range of different liquid conditions, and in
141 other replica measurements in liquid [29], support high reproducibility. In biofilms,
142 however, despite the fact that we did not bottleneck any population upon
143 inoculum, the poor correlation between replicas was evident (**Fig. 1b**). The
144 reproducibility between biological replicas indicates selection, suggesting that in
145 reproducible conditions, the fitness of *GudB*'s and of *B. subtilis* are tightly
146 coupled. In biofilms however, the lack of reproducibility suggested the
147 dominance of drift, *i.e.*, random sampling of GudB alleles.

148 To quantify the contribution of selection versus drift in different
149 conditions, we used two criteria. Firstly, we compared the variability in FC
150 values between replicas by calculating the standard deviation (SD) per allele
151 (using, by default, the logarithm of the FC values; see Methods). The average SD
152 value for all alleles in each experiment ($\overline{SD}$) is given for the different growth
153 states (a growth state, *e.g.* liquid, may include several conditions, *e.g.* different
154 carbon-nitrogen sources; **Fig. 1c; Fig. S3a** & **Table S2**). As can be seen, in liquid,
155 pellicles and spores, the $\overline{SD}$ values between biological replicas were low (< 0.06).
156 In biofilms and bulk soil, however, the $\overline{SD}$ values were > 0.25 indicating low
157 reproducibility. The Fisher test also indicated that for all tested alleles, the
158 variance between FC values significantly changed between liquid, pellicles and
159 spores when compared to germinated spores, biofilms and bulk soil (p values in
160 the range of 0.048 to 1.18×10^{-27}; **Data S2**).

161 Secondly, if drift dictates the fate of GudB alleles, codons of the same
162 amino acid should exhibit very different FC values. The deviations between

163 synonymous codon alleles of the same amino acid were calculated, averaged for
164 all alleles in the same experiment, and then for all replicas of the same
165 experiment ($\overline{SD}$syn, in log values; **Fig. 1d; Fig. S3b** & **Table S3**). The Levene's
166 test confirmed that the variance between synonymous codons is significantly
167 different across conditions (p values in the range of 0.01 to 10^{-24}; **Table S4**).
168 Note that the $\overline{SD}$syn criterion holds within individual replica experiments and is
169 thus independent of the comparison of $\overline{SD}$ between biological replicas.
170 Nonetheless, these criteria are clearly correlated (**Fig. 1c & d**). Overall, it appears
171 that in liquid, pellicles and spores, the FC values report the outcome of selection
172 acting on GudB alleles at the amino acid level as expected (in few alleles,
173 selection also acted reproducibly at the codon level, **Fig. S4**). In contrast, in
174 biofilms and bulk soil we consistently observed higher $\overline{SD}$ as well as higher
175 $\overline{SD}$syn values. In some biofilm experiments, in effect, a single codon had taken
176 over resulting in $\overline{SD}$syn values ≥ 3 (note that logFC values were compared
177 throughout, and the SD for FC values is therefore $\geq 10^3$).

178 Given that some conditions were selection-dominated and others were
179 subject to chance, we divided our analysis in two. Firstly, we analyzed selection
180 dominated conditions (liquid, pellicles and spores) to examine whether and how
181 GudB mutations exert different fitness effects under different environments.
182 Secondly, conditions where drift prevailed (germination, biofilms and soil
183 colonization) were analyzed to reveal the relative contributions of selection
184 *versus* chance.

185

186 **Pleiotropy - fitness-effects of mutations are condition-dependent**

187 While the FC values, and hence the fitness effects of mutations, were
188 reproducible under many conditions, their distribution varied widely between
189 conditions, including between carbon-nitrogen sources (**Fig. S5**). This indicates
190 pleiotropy – individual GudB alleles have different fitness effects in different
191 environments. To quantify the level of pleiotropy, we compared the FC values of
192 the same GudB mutation across the 9 individual selection-dominated conditions.
193 Because the number of generations differs from one condition to another, we
194 focused on shift from beneficial to deleterious, and vice versa (sign, or
195 antagonistic pleiotropy) because the sign indicates the overall trend irrespective
196 of generation numbers. Representative dot plots comparing the FC values across
197 3 different liquid conditions are shown (**Fig. 2a**). These indicate that pleiotropy
198 is common, even when comparing liquid cultures with overlapping carbon-
199 nitrogen sources. In particular, a significant number of GudB mutations show
200 antagonistic pleiotropy (dashed squares, **Fig. 2a**). Indeed, the Pearson
201 correlation values for the 36 possible pair-wise comparisons of the 9
202 reproducible conditions were all below 0.7, and many accommodated a negative
203 value indicating an overall anti-correlation (*i.e.*, dominance of antagonistic
204 pleiotropy; **Fig. 2b**). Across all selection-dominated conditions, 84% of alleles
205 showed antagonistic pleiotropy in at least one of the 36 pair wise comparisons,
206 and 70% of alleles showed mild or strong antagonistic pleiotropy. These
207 pleiotropic effects are far beyond experimental noise, as indicated by
208 comparison to a control sample (**Fig. 2c**).

209 Overall, the dominance of pleiotropy meant that across all conditions
210 where selection acts, 86% of the alleles were beneficial in at least one condition.
211 However, not a single mutation was beneficial across all conditions. Further, if a

212 mutation were to be considered deleterious if purged under at least one
213 condition, then 98% of the tested GudB mutations were deleterious.
214
215 **Combined action of selection and drift in heterogeneous environments**
216 In biofilms (and also in germination and soil colonization though to a lesser
217 degree), irreproducibility between replicas, variability between codons (**Fig. 1c**
218 & **d**), and the near-fixation of relatively few alleles (**Fig. 3**), all suggested fixation
219 by chance. What is the nature of these few GudB 'winners', are they merely
220 lucky?
221 While drift dominated in biofilms and soil colonization, curiously, wild
222 type GudB was enriched in up to 85% of these experiments suggesting that
223 selection may also play a role (**Fig. 3**). To assess the action of selection, we
224 compared the three biofilm areas. There appears a systematic trend, whereby
225 alleles enriched in the edge are more likely to arise from alleles that persisted or
226 even enriched in the center (**Fig. 4a**). Similarly, 75% of the enriched edge alleles
227 were neutral or beneficial under liquid growth with proline, a condition under
228 which GudB experiences the strongest selection (**Fig. 4b**). This suggested that
229 although drift dominated GudB's fate in biofilms, GudB was under selection at
230 some stage of biofilm development. Accordingly, we found that in biofilm centers
231 the FC values are less skewed and more reproducible than in the edge or
232 wrinkles (**Fig. S5b**) and the center $\overline{SD}$syn values are half (**Table S3** & **Fig. S3b**).
233 The $\overline{SD}$syn values are obviously much higher in the biofilms' center compared to
234 liquid cultures, but the trend suggests that at the onset of the biofilm's
235 development, selection acts on GudB (**Table S3** & **Fig. S3b**). Foremost, that wild
236 type GudB was present at high frequency in the vast majority of biofilm

experiments is not a coincidence that relates only to its high frequency in the initial mix. Indeed, a spiking experiment indicated that wild type was enriched by nearly 20-fold even when scarcely present in the initial mix (**Fig. 3f**).

Similarly, we searched signatures of selection in soil colonization – a process that involves multiple passages, beginning with a change of medium (Hoagland solution rinses; see Methods) and results in colonization of the roots. As in biofilms, there is a statistically significant trend whereby alleles enriched in the root are more likely to arise from alleles that were enriched in the soil (**Fig. 4c**). Further, 19 amino acid alleles were found to be enriched in at least 10 out of the 15 sequenced populations, suggesting some degree of reproducibility (**Table S5**). Selection during soil colonization is also manifested in the variation between biological replicas ($\overline{SD}$ values) of alleles that were enriched in root populations being on average 20% smaller than those that were not (**Fig. 4d**). Finally, stop codons were purged in all biofilms and soil populations, indicating, as expected, that GudB's activity is required for *B. subtilis'* survival under these conditions [22,23].

Altogether, in biofilms in soil colonization both drift and selection determine the fate of GudB alleles. We further examined the biofilms as described in the next section.

Drift in biofilms relates to programmed prophage excisions

Mutagenic rates in biofilms are high and mutations with a selective advantage rapidly take over (genetic sweeps) [30,31]. Growth in biofilms is also spatially defined, giving rise to segregated lineages whereby an entire segment of the biofilm's edge stems from a single cell in which a beneficial mutation had first

262 emerged [12]. GudB mutations that happen to be in these 'founder' cells might
263 therefore fixate along these lineages. In pellicles that are largely considered as
264 biofilms, intercellular matrix is produced [32] but spatial segregation is less
265 pronounced than in solid biofilms. Accordingly, we found that in oppose to agar
266 biofilms, in pellicles selection acts reproducibly (**Fig. 1**). To further establish that
267 spatial segregation is a key factor, we divided the edges of the biofilm into small
268 sections, and sequenced them. We found that most sections contained a single
269 GudB allele (**Fig. S6**). Thus, in a way, the GudB allele represents a 'barcode' that
270 reports single founder cells giving rise to individual sectors of the biofilm [12].

271 What might be the mutations driving these genetic sweeps and spatial
272 segregation? We sequenced samples for which enough genomic DNA was
273 available (6 ordinary and 12 gradient biofilms, and for comparison, 2 initial mix,
274 6 liquid and 4 pellicle samples). A range of single nucleotide polymorphisms
275 (SNPs) in various loci was identified across these samples (**Data S3**). We
276 focused, however, on identifying genomic mutations that were not, or scarcely
277 observed in the initial mix and/or in liquid samples, suggesting that they
278 emerged and enriched in the biofilms.

279 Foremost, we observed two large genome deletions that occurred in all
280 biofilms with a frequency approaching 100% (**Fig. 5a & 5b**). These deletions
281 correspond to the excision of two mobile genetic elements, or prophages, *skin*
282 and SP-β [33–35]. Excision of *skin* generates a functional protein: sigK - a
283 sporulation-specific transcription factor essential for cell differentiation in *B.*
284 *subtilis* [36]. The excision of SP-β generates another functional protein dubbed
285 SpsM – a protein involved in capsid polysaccharide biosynthesis mediating [37]
286 and with relevance to pellicle development [38]. Nearly all biofilm cells carried one

287 of these variations, and most cells carried both (**Fig. 5a & b**; **Table S6** & **Data**
288 **S3**). These prophage excisions therefore appear to be under stronger selection
289 than the GudB mutations. The frequency of these structural variations gradually
290 increases, from none in the initial mix to 100% in gradient biofilms (**Fig. 5c**), and
291 so does the signature of GudB's drift (**Fig. 1**). However, at this stage, the
292 observed link between the prophage excisions and GudB's drift is circumstantial
293 and further experiments are needed to establish how are these two phenomena
294 linked. The prophage excisions are also likely to occur in the soil, but the DNA
295 recovered from these samples was insufficient to allow genome sequencing.

296 Exclusively in biofilms, we also detected 59 enriched SNPs in a conserved
297 region of 16S rRNA (**Table S6** & **Data S3**). However, *B. subtilis* has ten 16S rRNA
298 gene copies. Since these are essentially identical, we could not determine which
299 of these 10 paralogues carried mutations. However, per population, 98% of the
300 16S rRNA mutations occurred in the same Illumina read suggesting that one
301 paralogue was highly mutated while others remained intact (**Fig. S7**). Large
302 differences in expression levels of 16S rRNA genes were identified *in P.*
303 *aeruginosa* biofilms [39], and ribosomal heterogeneity has been linked to biofilm
304 development in *B. subtilis* [40]. Yet, to our knowledge, mutations in the 16S rRNA
305 genes have not been reported in biofilms. At this stage, however, which 16S gene
306 is inactivated, how do multiple proximal 16S mutations occur, and how
307 inactivation affects biofilm development, remains unclear. Overall, the 16S rRNA
308 SNPs, and the structural variations in particular, seem to have a key role in
309 biofilm development in *B. subtilis*. Accordingly, most of these genetic variations
310 were reproducible between replica experiments (**Table S6**) suggesting that they

311 arose during biofilm growth and then enriched by virtue of promoting biofilm
312 formation [12].
313
314 **Concluding remarks**
315 That the fitness effect of a mutation may vary depending on the environment is
316 generally assumed. However, the magnitude of environmental pleiotropy
317 unraveled here is surprisingly high. Environmental changes, including minute
318 ones like addition of arginine to a proline medium, can completely revert the
319 effect of *GudB* mutations. Overall 84% of the tested GudB mutations showed sign
320 reversions. Pleiotropy severely restricts protein sequence space. Extensive
321 pleiotropy has an interesting implication. The so-called wild type sequence of a
322 gene-protein is generally thought to represent just one sequence out of an entire
323 cloud of related sequences that are similarly fit. However, our results indicate
324 that wild-type GudB's sequence is singular in being fit across multiple constrains
325 and environments. Per individual tested conditions, most mutations are either
326 neutral or beneficial (28 - 81%). However, if all tested conditions are considered,
327 only 2% of the tested GudB mutations are neutral or beneficial in the 9
328 reproducible conditions when selection acts on GudB.
329 The pleiotropy of protein mutations across multiple growth and
330 environmental conditions has been rarely measured [17], and, to our knowledge,
331 never for a protein with an intrinsic physiological role. Indeed, the extensive
332 pleiotropy observed here might be the norm in cases of complex relationships
333 between a protein's expression and activity levels ('protein fitness') and
334 organismal fitness, as with GudB. The high degree of pleiotropy observed here
335 may also relate to GudB's role as an enzyme and regulator, and also to the

336 positions explored (oligomer interface). In any case, our results suggest that, as
337 currently performed, laboratory mutational scans broadly underestimate the
338 fraction of mutations that are deleterious in 'real life'.

339 Together, pleiotropy and drift dictate not only the evolution of short-term
340 polymorphism (micro-evolution) but also the evolution of protein sequences
341 along long evolutionary times and across species (macro-evolution). Indeed, the
342 correlation between the effects of mutations in laboratory mappings and their
343 occurrence or absence in natural sequences is limited [13]. However, laboratory
344 mappings represent a single condition, and merging of data from multiple
345 conditions could in principle reveal higher correlation. Identifying trends in
346 complex datasets requires an unbiased approach. However, even when several
347 different machine learning approaches were applied, merging of conditions gave
348 no further correlation (**Fig. S8**). Thus, along short evolutionary periods, proteins
349 experience variable and opposing selection pressures. Additionally, drift may
350 lead to rapid fixation of alleles that are marginally fit or even deleterious. The
351 effects of drift have been extensively studied initiated by Kimura's neutral theory
352 [11]. Our results quantify its effect in bacterial populations and the potential effect
353 of drift in combination with selection across different environments. For
354 example, nearly 80% of the tested mutations survived or even enriched during
355 sporulation, and a single spore could then initiate a whole new population.
356 However, once the environment changes, such alleles will be rapidly lost unless
357 compensated or a priori enabled by other mutations. Compensation, or enabling
358 by other mutations, results in epistasis, i.e., in the effect of mutations being
359 dependent on the sequence context in which they occur [41]. Accordingly, along

macro-evolutionary time scales, epistasis dominates gene and genome sequences [42].

References

1. Baba, T. *et al.* Construction of Escherichia coli K-12 in-frame, single-gene knockout mutants: The Keio collection. *Mol. Syst. Biol.* **2,** (2006).
2. Koo, B. M. *et al.* Construction and Analysis of Two Genome-Scale Deletion Libraries for Bacillus subtilis. *Cell Syst.* **4,** 291–305.e7 (2017).
3. Pache, R. A., Madan, M. M. & Aloy, P. Exploiting gene deletion fitness effects in yeast to understand the modular architecture of protein complexes under different growth conditions. *BMC Syst. Biol.* **3,** (2009).
4. Winzeler, E. A. *et al.* Functional characterization of the S. cerevisiae genome by gene deletion and parallel analysis. *Science (80-.).* **285,** 901–906 (1999).
5. Civelek, M. & Lusis, A. J. Systems genetics approaches to understand complex traits. *Nature Reviews Genetics* **15,** 34–48 (2014).
6. Steinberg, B. & Ostermeier, M. Environmental changes bridge evolutionary valleys. *Sci. Adv.* **2,** e1500921 (2016).
7. Wang, Z., Liao, B.-Y. & Zhang, J. Genomic patterns of pleiotropy and the evolution of complexity. *Proc. Natl. Acad. Sci.* **107,** 18034–18039 (2010).
8. Fusco, D., Gralka, M., Kayser, J., Anderson, A. & Hallatschek, O. Excess of mutational jackpot events in expanding populations revealed by spatial Luria-Delbrück experiments. *Nat. Commun.* **7,** (2016).
9. Kimura, M. Genetic variability maintained in a finite population due to mutational production of neutral and nearly neutral isoalleles. *Genet. Res. (Camb).* **89,** 341–363 (2008).
10. Smith, N. H., Gordon, S. V., de la Rua-Domenech, R., Clifton-Hadley, R. S. & Hewinson, R. G. Bottlenecks and broomsticks: The molecular evolution of Mycobacterium bovis. *Nature Reviews Microbiology* **4,** 670–681 (2006).
11. Nei, M. Selectionism and neutralism in molecular evolution. *Molecular Biology and Evolution* **22,** 2318–2342 (2005).
12. Steenackers, H. P., Parijs, I., Foster, K. R. & Vanderleyden, J. Experimental evolution in biofilm populations. *FEMS Microbiology Reviews* **40,** 373–397 (2016).
13. Boucher, J. I., Bolon, D. N. A. & Tawfik, D. S. Quantifying and understanding the fitness effects of protein mutations: Laboratory versus nature. *Protein Science* 1219–1226 (2016). doi:10.1002/pro.2928
14. De Visser, J. A. G. M. & Krug, J. Empirical fitness landscapes and the predictability of evolution. *Nature Reviews Genetics* **15,** 480–490 (2014).
15. Fowler, D. M. & Fields, S. Deep mutational scanning: A new style of protein science. *Nature Methods* **11,** 801–807 (2014).
16. Steinberg, B. & Ostermeier, M. Shifting Fitness and Epistatic Landscapes Reflect Trade-offs along an Evolutionary Pathway. *J. Mol. Biol.* **428,** 2730–2743 (2016).
17. Dandage, R. *et al.* Differential strengths of molecular determinants guide environment specific mutational fates. *PLoS Genet.* **14,** (2018).
18. Earl, A. M., Losick, R. & Kolter, R. Ecology and genomics of Bacillus subtilis. *Trends in Microbiology* **16,** 269–275 (2008).
19. Branda, S. S., González-Pastor, J. E., Ben-Yehuda, S., Losick, R. & Kolter, R. Fruiting body formation by Bacillus subtilis. *Proc. Natl. Acad. Sci. U. S. A.* **98,** 11621–6 (2001).

411 20. Belitsky, B. R. & Sonenshein, A. L. Role and regulation of Bacillus subtilis
412 glutamate dehydrogenase genes. *J. Bacteriol.* **180,** 6298–305 (1998).
413 21. Gunka, K. & Commichau, F. M. Control of glutamate homeostasis in Bacillus
414 subtilis: A complex interplay between ammonium assimilation, glutamate
415 biosynthesis and degradation. *Molecular Microbiology* **85,** 213–224
416 (2012).
417 22. Liu, J. *et al.* Metabolic co-dependence gives rise to collective oscillations
418 within biofilms. *Nature* **523,** 550–554 (2015).
419 23. Noda-Garcia, L., Romero Romero, M. L., Longo, L. M., Kolodkin-Gal, I. &
420 Tawfik, D. S. *Bacilli* glutamate dehydrogenases diverged via coevolution of
421 transcription and enzyme regulation. *EMBO Rep.* **18,** 1139–1149 (2017).
422 24. De Jong, L. *et al.* In-Culture Cross-Linking of Bacterial Cells Reveals Large-
423 Scale Dynamic Protein-Protein Interactions at the Peptide Level. *J.*
424 *Proteome Res.* **16,** 2457–2471 (2017).
425 25. Stannek, L. *et al.* Evidence for synergistic control of glutamate biosynthesis
426 by glutamate dehydrogenases and glutamate in Bacillus subtilis. *Environ.*
427 *Microbiol.* **17,** 3379–3390 (2015).
428 26. Mondal, S., Yakhnin, A. V., Sebastian, A., Albert, I. & Babitzke, P. NusA-
429 dependent transcription termination prevents misregulation of global
430 gene expression. *Nat. Microbiol.* **1,** (2016).
431 27. Besharova, O., Suchanek, V. M., Hartmann, R., Drescher, K. & Sourjik, V.
432 Diversification of gene expression during formation of static submerged
433 biofilms by Escherichia coli. *Front. Microbiol.* **7,** (2016).
434 28. Vlamakis, H., Chai, Y., Beauregard, P., Losick, R. & Kolter, R. Sticking
435 together: Building a biofilm the Bacillus subtilis way. *Nature Reviews*
436 *Microbiology* **11,** 157–168 (2013).
437 29. Mavor, D. *et al.* Determination of ubiquitin fitness landscapes under
438 different chemical stresses in a classroom setting. *Elife* **5,** (2016).
439 30. Nguyen, D. & Singh, P. K. Evolving stealth: genetic adaptation of
440 Pseudomonas aeruginosa during cystic fibrosis infections. *Proc. Natl. Acad.*
441 *Sci. U. S. A.* **103,** 8305–8306 (2006).
442 31. Hallatschek, O., Hersen, P., Ramanathan, S. & Nelson, D. R. Genetic drift at
443 expanding frontiers promotes gene segregation. *Proc. Natl. Acad. Sci.* **104,**
444 19926–19930 (2007).
445 32. Lemon, K. P., Earl, A. M., Vlamakis, H. C., Aguilar, C. & Kolter, R. Biofilm
446 development with an emphasis on Bacillus subtilis. *Current Topics in*
447 *Microbiology and Immunology* **322,** 1–16 (2008).
448 33. Kunkel, B., Losick, R. & Stragier, P. The Bacillus subtilis gene for the
449 developmental transcription factor σ(K) is generated by excision of a
450 dispensable DNA element containing a sporulation recombinase gene.
451 *Genes Dev.* **4,** 525–535 (1990).
452 34. Nicolas, P. *et al.* Condition-dependent transcriptome reveals high-level
453 regulatory architecture in Bacillus subtilis. *Science (80-.).* **335,** 1103–1106
454 (2012).
455 35. Westers, H. *et al.* Genome Engineering Reveals Large Dispensable Regions
456 in Bacillus subtilis. *Mol. Biol. Evol.* **20,** 2076–2090 (2003).
457 36. Eichenberger, P. *et al.* The program of gene transcription for a single
458 differentiating cell type during sporulation in Bacillus subtilis. *PLoS Biol.* **2,**
459 (2004).

37. Abe, K. *et al.* Developmentally-Regulated Excision of the SPβ Prophage Reconstitutes a Gene Required for Spore Envelope Maturation in Bacillus subtilis. *PLoS Genet.* **10,** (2014).
38. Martin, M. *et al.* De novo evolved interference competition promotes the spread of biofilm defectors. *Nat. Commun.* **8,** (2017).
39. Pérez-Osorio, A. C., Williamson, K. S. & Franklin, M. J. Heterogeneous rpoS and rhlR mRNA levels and 16S rRNA/rDNA (rRNA Gene) ratios within Pseudomonas aeruginosa biofilms, sampled by laser capture microdissection. *J. Bacteriol.* **192,** 2991–3000 (2010).
40. Vesper, O. *et al.* Selective translation of leaderless mRNAs by specialized ribosomes generated by MazF in Escherichia coli. *Cell* **147,** 147–157 (2011).
41. Miton, C. M. & Tokuriki, N. How mutational epistasis impairs predictability in protein evolution and design. *Protein Sci.* 1260–1272 (2016). doi:10.1002/pro.2876
42. Breen, M. S., Kemena, C., Vlasov, P. K., Notredame, C. & Kondrashov, F. A. Epistasis as the primary factor in molecular evolution. *Nature* **490,** 535–538 (2012).
43. Konkol, M. A., Blair, K. M. & Kearns, D. B. Plasmid-encoded comi inhibits competence in the ancestral 3610 strain of Bacillus subtilis. *J. Bacteriol.* **195,** 4085–4093 (2013).
44. Yi, Y., de Jong, A., Frenzel, E. & Kuipers, O. P. Comparative transcriptomics of Bacillus mycoides root exudates reveals different genetic adaptation of endophytic and soil isolates. *Front. Microbiol.* **8,** (2017).
45. Deatherage, D. E. & Barrick, J. E. Identification of mutations in laboratory-evolved microbes from next-generation sequencing data using breseq. *Methods Mol. Biol.* **1151,** 165–188 (2014).

Acknowledgments

L.N.G. was supported by the CONACYT grant #203740 and the Martin Kushner Fellowship at the Weizmann Institute of Science. D.S.T. is the Nella and Leon Benoziyo Professor of Biochemistry. Financial support by the Kahn Center for Systems Biology at the Weizmann Institute of Science is gratefully acknowledged. We are highly grateful to Ron Milo, Sarel Fleishman, Zvi Livneh and Fyodor Kondrashov for support and critical advice, to Einat Segev, Arjan de Visser for critical and insightful comments to the manuscript. We highly appreciate the help of Moshe Hershko in script development for data processing, and of Yinon Bar-On, Shmuel Gleizer in the analysis of genomic sequences. We

are grateful to Ron Rotkopf from the Weizmann Life Sciences Core Facilities for his guidance on the statistical analysis. We are thankful for the services provided by the Crown Genomics institute of the Nancy and Stephen Grand Israel National Center for Personalized Medicine, Weizmann Institute of Science.

Authors Contribution

L.N.G. and D.S.T. designed experiments and wrote the manuscript. L.N.G., D.D. and D.S.T. analysed the data. L.N.G. performed all experiments, except selection in soil colonization that was performed in collaboration with E.K. and A.A. D.D. and A.E. wrote the scripts used for data analysis and visualization. E.P. applied machine learning classification.

510 **Fig. 1. Selection *versus* chance-dominated conditions. (A)** Dot-plot indicating
511 reproducible measurements of frequency coefficients of individual mutations
512 (FC values) in three parallel replica liquid cultures with proline as carbon-
513 nitrogen source. $\overline{SD}$ is the average standard deviation between 3 biological
514 replicas. The S.D. values were calculated per each amino acid allele based on
515 logFC values and averaged for all alleles in a given condition. **(B)** The same
516 analysis of three parallel biofilms with arginine as carbon-nitrogen source
517 indicates low reproducibility. **(C)** The $\overline{SD}$ values categorized by the 7 general
518 growth states tested here. Each point represents the $\overline{SD}$ value between 3 replicas
519 of the same experiment (the distributions of SD values per each condition are
520 shown in **Fig. S3a**). **(D)** $\overline{SD}$syn represents the standard deviation between the
521 logFC values of synonymous codons. The standard deviations per allele were
522 averaged for all synonymous alleles in the same replica experiment, and then
523 averaged across the 3 replica experiments in a given condition (the distributions
524 of SD*syn* values per experiment are shown in **Fig. S3b**).
525

526 **Fig. 2. The pleiotropic effects of alleles across different conditions.** (**A**) A
527 dot-blot correlation of FC values of individual alleles in three different liquid
528 carbon-nitrogen sources (average values per 3 replicas). The red squares
529 encompass alleles that show sign pleiotropy – i.e., a change from beneficial to
530 deleterious, or vice versa. (**B**) Pairwise correlation of the FC values in all 9
531 different reproducible conditions (3 replicas per condition; average FC values of
532 all alleles and replicas). Colors indicate the Pearson correlation values (-1,
533 negative correlation; 0, no correlation; 1, positive correlation). The strongest
534 anti-correlation was found with arginine as carbon-nitrogen source (black
535 square). (**C**) The distribution of alleles by their level of sign pleiotropy; from pale
536 to dark purple: (*i*) Weak sign pleiotropy (changes between deleterious and
537 beneficial); (*ii*) Mild sign pleiotropy (changes from highly deleterious to
538 beneficial, or from highly beneficial to deleterious); and (*iii*) Strong sign
539 pleiotropy (changes from highly deleterious to highly beneficial, or vice versa).
540 The fraction of alleles showing mild or strong sign pleiotropy is shown above the
541 bars. The control dataset comprises 4 completely independent growth
542 experiments in liquid proline, each inoculated from a different initial mix and
543 grown on separate occasions (**Fig. S9**). Nonetheless, none of the alleles in this
544 control set exhibited strong pleiotropy. Accordingly, a Chi-squared analysis
545 indicated that the variations between conditions are significantly higher than the
546 variations in the control group (X^2 and p values are shown; degrees of freedom
547 equal 3 in all cases).
548

549 **Fig. 3. Genetic sweeps in biofilms and soil and the dominance of the wild-**
550 **type allele.** Photographs of 5 days old biofilms: (**A**) normal biofilms; (**B**)
551 gradient biofilms; (**C**) a scheme of soil colonization (shown biofilms with proline
552 as carbon-nitrogen source). (**D**) The distribution of frequency of individual
553 alleles for different growth states with proline as carbon-nitrogen source. Bar
554 widths represent allele frequency from raw read counts (Rf values**; Data S1**).
555 Magenta corresponds to wild type GudB. (**E**) Alleles with Rf ≥ 1% were identified
556 and their number and sum of frequencies are shown (averages and standard
557 deviations for all experiments in a given condition). Blue designates selection-
558 dominated conditions and red drift-dominated ones, as in **Fig. 1**. (**F**) An initial
559 mix of 4 alleles was created including the wild-type allele at a varying frequency
560 from 1 up to 25%. Following growth in normal and gradient biofilm with proline,
561 the frequency of wild-type reached an average of 18% when initiated at 1%, and
562 up to 100% when initiated at 5% (see **Fig. S10** for the entire dataset).
563

Fig. 4. The combined action of selection and chance in biofilms (red) and soil colonization (green). (A) Alleles that enriched in the edge of the biofilms are more likely to arise from alleles that were neutral or enriched in the center. The distribution of categorized FC values from all biofilm centers (grey) compared to the distribution of FC values of center alleles that were enriched in the edge (red). **(B)** The distribution of categorized FC values of all alleles in all liquid conditions (grey) compared to the distribution of FC values of liquid alleles that were enriched in the edge of biofilms (red). **(C)** Alleles enriched in the root are more likely to arise from alleles that were enriched in the bulk soil. The distribution of categorized allele FC values in all soil samples (grey) compared to the distribution of FC values of soil alleles that were enriched in the root (green). **(D)** The distribution of SD values (variability between replica experiments, as in **Fig. 1c**) of alleles enriched in one or more root populations compared to alleles that were never enriched in the roots. T-tests were computed per each FC category. p-values indicating significance ($p < 0.05$) are presented above the bars (details of all the T-tests are provided in **Table S7**).

581 **Fig. 5. Programmed genomic excisions drive GudB's drift in biofilms.**
582 Schematic representation of *B. subtilis* genomic organization before and after the
583 excision of the prophage mobile elements SP-β (**A**) and *skin* (**B**) and their
584 position in the genome. (**C**) These excisions were absent in the initial mix yet
585 dominated biofilms and went to near fixation in the edge of gradient biofilms (for
586 frequencies in individual experiments see **Table S6**). Excision of the mobile
587 elements occurred in two different genomic locations within the same
588 experiment. The values were summed and averaged according to the general
589 condition shown. The details of the excisions (location and frequency) per
590 experiment are shown in **Data S3**.
591

592 **Materials and Methods**

593 **Strains**

594 *B. subtilis* NCIB 3610 DS7187 (kindly gifted by Dr. Daniel B. Kearns [43]) that lacks
595 the ComI peptide and has high competence capacity similar to domesticated *B.*
596 *subtilis* strains was recruited to this study. *Bacillus subtilis* NCIB 3610 *gudB::tet*
597 strain [23] genomic DNA was transformed into *B. subtilis* NCIB 3610 DS7187. *B.*
598 *subtilis* NCIB 3610 *ΔcomI gudB::tet* was thus isolated, and was phenotypically
599 and genetically tested.

600

601 **GudB allele library construction**

602 We performed site directed mutagenesis in 10 codons (amino acids: M46, L48,
603 K52, D58, D59, S61, K63, T66, Y68, S75) of the *gudB* gene cloned in the
604 pDG_GudB plasmid, which was modified from the pDG1728 backbone vector [23].
605 The codons were mutated to NNS (N = all bases & S = C or G) whereby the 20
606 standard amino acids and 1 stop codon is encoded. The codon mutagenesis was
607 done in one step PCR protocol and independently for each position. Thus, we
608 created 10 libraries, each containing 20 different amino acid alleles (non-
609 synonymous, missense mutations), 1 stop-codon (nonsense), and 11
610 synonymous alleles (alternative codons encoding the same amino acid). All
611 mutagenic PCRs were performed with Kapa HiFi HotStart Ready Mix (Kapa
612 Biosystems) following manufacturers conditions (**Table S8** shows the sequence
613 of all primers). The 10 PCR products were purified and used to transform the *E.*
614 *coli* T10 strain (Thermo Fisher Scientific). Clones were pulled together after an
615 overnight growth on LB + Ampicillin (100 μg/ml) agar plates at 37°C. At this
616 stage, 4 to 6 clones per library were isolated and analyzed by sequencing. Total
617 plasmid DNA from these library transformations was extracted and also
618 analyzed by sequencing. Each of the 10 libraries contained, after transformation,
619 at least 10^5 clones, corresponding to ≥ 1000-fold coverage per allele.
620 Approximately 10 μg of plasmid DNA, from each library, was linearized (XhoI,
621 New England Biolabs, following manufactures conditions), purified, and used to
622 transform the *B. subtilis* NCIB 3610 *gudB::tet ΔcomI* strain. Transformations were
623 performed as described [23]. After transformation, overnight growth on in +
624 Spectinomycin (100μg/ml) + Glucose (0.5 mg/ml) agar plates was used as

625 selection. The resulting cells were pulled together and kept at -20°C in 50%
626 glycerol. In total, 10 *B. subtilis* libraries were constructed in parallel and each
627 contained, after transformation, at least 10^4 clones (≥100-fold coverage per
628 allele). Genomic DNA extraction of each library was performed (GenElute -
629 Sigma). The integrity of the mutagenic process was verified by sanger
630 sequencing the *amyE::gudB* locus indicating that mutations were observed only
631 in the diversified codon.
632
633 **Selection and growth conditions**
634 10 ml of LB (1% tryptone, 5% yeast extract and 1% NaCl) with Glucose (0.5%),
635 ammonium sulfate (0.5%) and spectinomycin (100 µg/ml) cultures were
636 inoculated with 1 ml of each library stock. The cultures were grown overnight at
637 37°C with shaking. 500 µl of the overnight culture was used to inoculate 3 ml of
638 LB plus glucose (0.5%) and ammonium sulfate (0.5%). The cultures were
639 incubated at 37°C with shaking and once the $O.D._{600}$ reached 0.8 they were mixed
640 equally and used as the starting population (initial mix). A fraction of the cells at
641 this stage were harvested by centrifugation and stored for genomic DNA
642 purification. In total, three different initial mixes were used for the experiments
643 described here. Initial Mix #1 was used to inoculate most liquid conditions (4
644 carbon-nitrogen sources), pellicles and gradient biofilms. Initial Mix #2 was used
645 to inoculate 1 liquid condition, spores, germination and biofilms, and initial mix
646 #3 was used to inoculate bulk soil (**Data S1**). Detailed selection conditions are
647 listed below:
648 For selection under liquid serial passages 100 ul of the initial mix was used to
649 inoculate 10 ml cultures of MS medium (5 mM potassium phosphate, 100 mM
650 MOPS pH 7.1, 2 mM $MgCl_2$, 700 µM $CaCl_2$, 50 µM $MnCl_2$, 50 µM $FeCl_3$, 1 µM $ZnCl_2$,
651 2 µM thiamine, 50 µg/ml tryptophan, 50 µg/ml phenylalanine and 50 µg/ml
652 threonine)[23] with glucose (0.5%) plus ammonium sulfate (0.5%), glutamate
653 (0.5%) plus glycerol (0.5%), proline (0.5%), arginine (0.5%) or proline (0.25%)
654 plus arginine (0.25%). The cultures were incubated at 30°C with shaking until
655 $O.D._{600}$ reached 1 – 1.5, after which 100 µl was used to inoculate 10 mL of fresh
656 medium. The serial passages were done every 24 hours when proline (0.5%),
657 arginine (0.5%) or proline (0.25%) plus arginine (0.25%) where used as carbon-

658 nitrogen sources, and every 12 hours when glucose (0.5%) plus ammonium
659 sulfate (0.5%), or Glutamate (0.5%) plus glycerol (0.5%), were applied. In total,
660 all liquid passages were maintained for approximately 50 generations.
661 For selection in pellicles, 100 ml of media (b), (c) and (d) were inoculated with
662 100 µl of the initial mix cells. The culture was incubated at 30°C without shaking,
663 for 5 days.
664 For selection of spores and germinated spores, three ml of the initial mix was
665 used to inoculate 25 ml of Difco Sporulation Medium (DSM) in 250 ml flasks and
666 incubated at 37°C with 150 rpm shaking until O.D.600 reached 0.4. This culture
667 was used to inoculate 250 ml of fresh DSM in 1L flasks. The cultures were
668 incubated 48h at 37°C with 150 rpm shaking. Cells were subsequently harvested
669 by centrifugation and stored at 4°C over night. After, cells were re-suspended
670 with 200 ml of cold deionized sterile water (dW) and incubated for 30 min at
671 4°C. Cells were harvested and re-suspended with 200 ml of cold distilled water
672 (dW) and incubated overnight at 4°C with slow orbital agitation, to kill all
673 planktonic of vegetative cells. The culture was harvested, re-suspended in 30 ml
674 of dW and heated to 80°C for 20 min. Finally, spores were harvested, re-
675 suspended in 10 ml of dW, and stored at -20°C. To germinate these spores, they
676 were diluted 1000 times in phosphate-buffered saline solution and 100 µl of this
677 suspension was used to inoculate LB plus glucose (0.5%) agar plates (10 plates).
678 Approximately 10,000 colonies were obtained and pulled together.
679 For selection in biofilms, MS agar (1.5%) plates supplemented with different
680 carbon-nitrogen sources were prepared. For gradient biofilms, gradient agar
681 plates were prepared. First, square plates (12x12 cm) with MS agar (1.5%)
682 medium were poured. After the agar solidified, an area of 2x14 cm was removed
683 from the top of the plate. In this area, a solution of either Proline 5%, Arginine
684 5%, monosodium glutamate 5% or Glycerol 5% in 1.5% agar was poured into
685 the removed section. For the glutamate plus glycerol gradient biofilm, two
686 opposite areas of the agar plate were removed. Into one, a solution of
687 monosodium glutamate (5%) in 1.5% agar was poured, and into the other,
688 glycerol (5%) plus 1.5% agar solution (see **Fig. S11a** for a graphic
689 representation of the agar plates preparation). All gradient agar plates were
690 incubated for 24 h at room temperature before use. We also calibrated the place

691 in the gradient plate where we inoculated the cells such that we observed
692 growth after 1 night incubation at 30°C (**Fig. S11b**). For growth in biofilms and
693 gradient biofilms, 5 µl of the initial mix were used as inoculum. Plates were
694 incubated for 4 days at 30°C and 2 more days at room temperature. The colony
695 was then dissected in 3 areas (center, wrinkle and edge) for normal biofilms, and
696 in 2 areas (center and upper) for gradient biofilms (illustrated in **Fig. S11c-g**).
697 After selection in all the above-mentioned conditions the biomass was harvested
698 and storage at -20°C. All growth experiments were performed in triplicate by
699 inoculating with the same initial mix.
700 For selection in soil and plant roots, the initial mix was generated as above-
701 mentioned except that the process was scaled up (instead of 3 ml, 10 ml of
702 culture was prepared per library). In total, 200 ml of the initial mix ($O.D._{600}$ = 0.8)
703 was applied. This LB culture was washed three times (by means of centrifugation
704 and re-suspension) with 100 ml half strength Hoagland solution [44]. After the final
705 wash, the cells were re-suspended in half strength Hoagland solution to a final
706 $O.D._{600}$ of 0.1. Since Hoagland's solution is not isotonic, the washes resulted in
707 death of about a third of the *B. subtilis* cells. Thus, handling the samples at this
708 stage was performed as fast as possible. The Hoagland solution imposes some
709 selection pressure on the initial mix population although the loss in population
710 size is relatively small (≤30%). The soil colonization FC values therefore result
711 from the entire process that begins the rinses with the Hoagland solution and
712 ends with the colonization of the roots. Natural soil was collected at the Ha-
713 Masrek Reserve, Israel (31.793 N, 35.042 E), sifted through 2 mm sieve and
714 autoclaved three times for 30 min at 121°C. A total of five pots (size 10 x 8 x 5
715 cm) with autoclaved natural soil were drenched with the initial mix suspended in
716 half strength Hoagland Solution [44]. These potted soils drenched with bacterial
717 suspensions were used to plant tomato seedlings grown first in sterile
718 conditions. Seeds of tomato (*Solanum lycopersicum L.*; cv. Micro-Tom) were
719 surface-sterilized with 70% ethanol for 5 minutes and, 10 minutes with 3%
720 bleach with 0.01% Tween 20. Surface-sterile seeds were germinated on sterile
721 filter paper (Whatman, catalog # 1001-085) saturated with half strength
722 Hoagland Solution for 7 days (23°C and 16 hours photoperiod). Six tomato
723 seedlings were transferred to each pot and grown for one month (21°C, 16h

724 light, 8h dark) with drenching with half strength Hoagland twice a week. Plants
725 were subsequently harvested from the five pots. Roots and rhizosphere samples
726 were collected for each replica experiment consisting a pool of six roots. First,
727 the plants were carefully removed from the soil. Roots were then cut out from
728 the plants and vortexed in 20 ml of washing solution (0.85% NaCl) for 30 s. This
729 step was repeated one more time with a fresh washing solution. The combined
730 root washing solutions (40 ml) was centrifuged for 30 min at 3000 rpm and the
731 resulted pelleted samples corresponding to the rhizosphere were frozen in liquid
732 nitrogen and stored at -80°C. The washed roots were blotted in filter paper and
733 stored at −80°C until further use. Finally, bulk soil without roots was also stored
734 at −80°C.
735
736 **Genomic DNA extraction**
737 All samples, including pellicle, spores, biofilm and gradient biofilm samples, were
738 defrosted and re-suspended in 10 ml of dW. The samples were sonicated at 40%
739 power, VibraCell, Sonics, for 10 min at 60 s intervals. Cells debris was harvested
740 by centrifugation (13,000 g for 20 min). Genomic DNA from all samples was
741 extracted using the GenElute Bacterial Genomic DNA Kit (Sigma-Aldrich)
742 generally following the manufacturer's instructions, with the exception of the
743 soil, rhizosphere soil and plant roots samples. For these samples, the PowerSoil
744 DNA Isolation kit of Mo Bio was used, following its manufacturer's instructions.
745
746 **Illumina sample preparations**
747 The mutagenized *gudB* fragment (from amino acids 45 to 81) was amplified
748 using the primers GudB_In_For (5'-
749 CTCTTTCCCTACACGACGCTCTTCCGATCTnnnnnnCCCGAAGAGGTATACGAATTGT
750 TAAAAGAG), and GudB_In_Rev (5'-
751 CTGGAGTTCAGACGTGTGCTCTTCCGATCTCGCCTTTCGTTGGACCGAC). To the
752 GudB_In_For primer, 6 N's were added to increase the sequence variability
753 between amplicons. PCRs were performed with the KapaHiFi HotStart Ready Mix
754 (Kapa Biosystems) using approximately 100 ng of genomic DNA as template and
755 following manufacturer's instructions. Using 10 µl of the PCR as template, a
756 second PCR was performed to add the Illumina adaptor sequence, using primers

757 GudB_Out_For (5'-
758 AATGATACGGCGACCACCGAGATCTACACTCTTTCCCTACACGACGC) and
759 GudB_Out_Rev (5'-
760 CAAGCAGAAGACGGCATACGAGATTGTTATACGTGACTGGAGTTCAGACGTGTGC).
761 The Illumina index (underlined) was changed in the GudB_Out_Rev primer to
762 different Illumina indexes. Each condition was differently barcoded. All PCRs
763 were purified using the Agencourt AMPure XP (Beckman Coulter). The
764 concentration of PCR products was verified using Qu-bit assay (Life
765 Technologies).
766
767 **Analysis of the Illumina reads**
768 DNA samples were run using the Illumina NextSeq 150-bp paired-end kit. The
769 FASTQ sequence files were obtained for each run and customized using MatLab
770 8.0 and Python 3.6 scripts designed to count the number of each individual allele
771 in each sequenced sample. We filtered the reads to exclude any reads that have
772 mutations outside the mutagenized codons. All codons encoding for the wild-
773 type amino acid were summed in one and assigned as WT. All other codons were
774 counted independently. The unprocessed read counts are shown in **Data S1**.
775 Further filtering excluded alleles with < 100 counts in the initial mix to avoid
776 statistical uncertainty with respect to FC values. In total, we obtained data for up
777 to 269 individual alleles per condition out of the originally introduced 320
778 alleles. Per condition, a minimum of 380,000 reads was obtained. Thus, in
779 average, we obtained 1500 reads per allele.
780
781 **Data Analysis**
782 The frequency of each allele (f_i) was calculated as the ratio between the number
783 of reads for allele i divided by the total number of reads. The allele frequency
784 coefficient (FC_i) was subsequently calculated as the ratio of after selection (f_i)
785 divided by the frequency of the same allele in the initial mix (**Fig. S2** & **Data S2**).
786 Normalization by the number of wild-type reads rather than by the total number
787 of reads gave essentially identical FC values for the majority of samples.
788 However, in the few samples where wild-type frequency was significantly
789 reduced after selection, normalization resulted in high noise and large biases

790 including large changes in sign (higher sign pleiotropy). FC values were
791 therefore derived from the unnormalized frequency (fraction of reads for a given
792 allele out of the total number of reads). FC values relate to fitness
793 logarithmically, and thus logFC values were compared. To this end, all FC's equal
794 to zero had to be changed, and we opted for a tenth of the minimum FC value
795 found amongst all experiments. For the liquid, pellicles, biofilms, spores and
796 germinated spores experiments (**Data S2, sheet 1**) the zeros were changed to
797 4.2×10^{-6}. For the bulk soil experiments (**Data S2, sheet 2**) zeros were changed
798 to 1.14×10^{-5}. The logarithm of all FC values was calculated and was also used to
799 derive mean FC values. The logFC values were then used to calculate: (i) the
800 standard deviation for all alleles across conditions ($\overline{SD}$; the standard deviation
801 between logFC values observed per each allele in replica experiments were
802 averaged for all alleles measured in a given condition); (ii) the standard
803 deviation between synonymous codons within the same replica experiment
804 (deviations between logFC values of synonymous codons of the same amino acid
805 allele were calculated, averaged for all alleles in the same experiment, and then
806 for all replica experiments per condition). The T, F, X^2 tests and Pearson
807 correlation values were obtained using the PRISM software. The Levene's test
808 was performed using R. In addition, **Table S9** from supplementary material
809 shows the sample size for every test performed in this study.
810
811 **Defining the limits of neutrality**
812 From all conditions tested here, only in glucose plus ammonia the GudB
813 knockout had no growth effect (**Fig. S1**). Hence, this condition is largely neutral,
814 and the variation observed in FC values would primarily be the outcome of noise.
815 The standard deviation between 3 biological replicas was calculated per allele,
816 and these values spanned over the range of 0.002 to 0.199. We rounded this
817 number to 0.2. Thus, by the strictest measure, FC values between 0.8 and 1.2
818 were classified as 'neutral'. Accordingly, FC ≤0.8 unambiguously assigned a
819 mutation as 'deleterious', and FC >1.2 as 'beneficial'.
820
821 **Genome sequencing**

822 We sequenced the genomic DNA of all biofilm populations for which we had ≥ 1
823 μg of DNA after extraction (6 normal and 12 gradient biofilm). For comparison,
824 we also sequenced initial mix populations 1 and 2, 6 Liquid and 4 pellicle
825 populations. The Illumina HiSeq2500 platform was used, with 2x125 base pairs
826 read length. We obtained a total of 300 million reads. The reads were assembled
827 using as reference the *B. subtilis* NCIB 3610 genome (NCBI Accession number:
828 CP020102). Overall, 95% of all reads were successfully mapped to the reference
829 genome with minimal coverage of x300 for all samples analyzed. The Breseq
830 program was used to identify genomic variants, including single nucleotide
831 polymorphisms (SNPs) and insertion-deletion polymorphisms (INDELs) [45] (**Data**
832 **S3** & **Table S6**).
833
834 **Comparison of FC values and to GudB's natural sequence variability**
835 We examined whether the FC values for individual mutations, in individual
836 conditions, and in combinations thereof, might predict whether or not a certain
837 sequence exchange is observed, or not, amongst the sequences of naturally
838 occurring GDHs. To this end, we constructed a number of different support
839 vector machines (SVM) classification models with a variety of kernels (such as
840 linear, Gaussian, polynomial etc.). The feature vector of each GudB allele was
841 composed from the normalized FC values from specific condition. The values
842 from replica experiments of the highly reproducible liquid conditions were
843 averaged prior to training. Based on the multiple sequence alignment containing
844 1013 GDH sequences, we divided the GudB mutations in our dataset into 3
845 categories, which were then utilized as the prediction labels: (1) mutations seen
846 in less than 5 natural GDH sequences (classified as 'not present', 66% of
847 mutations), (2) mutations observed in 5 - 49 sequences ('rare', 19%) and (3)
848 mutations present in ≥50 sequences ('frequent', 15%). Introducing class weights
849 into the loss function compensated the unbalanced nature of the dataset. For
850 each feature combination of a varied length, we built an SVM classification model
851 and assessed its accuracy using 3-fold cross validation. Additionally, in order to
852 reduce noise, assuming that our data belong to linear space, we extracted the
853 first ten principal components of the feature matrix and used them as the new
854 feature vectors for a model construction. To examine if our relatively high (>0.6)

model accuracy was distributed uniformly across different classes, for each model and genotype, we recorded the predicted values during 3-fold cross-validation. Moreover, for each condition combination, and for each kernel, we built 100 different models and recorded the number of times each of the genotypes was predicted correctly.

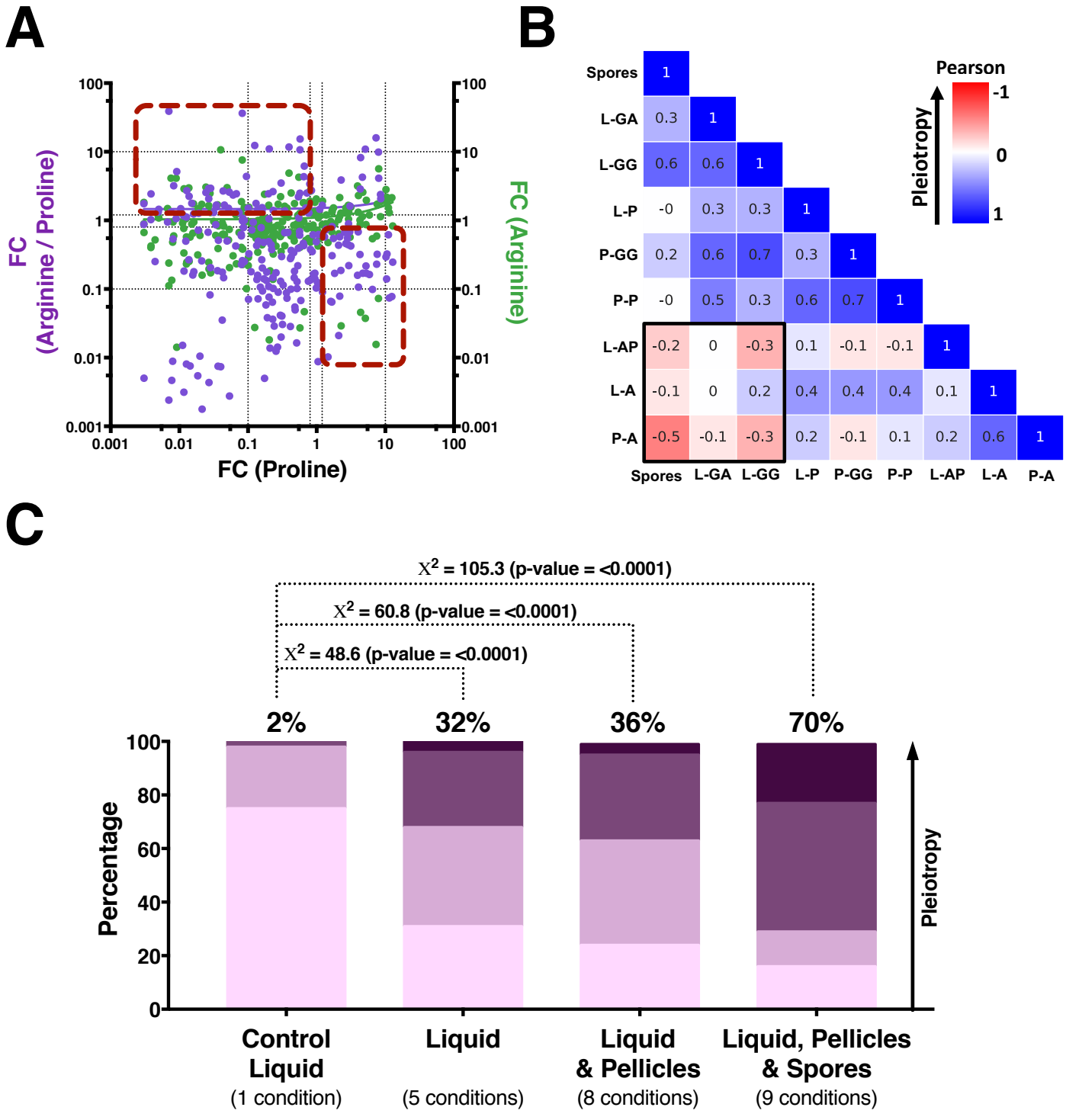
A
FC (Arginine / Proline)
FC (Arginine)
FC (Proline)
100
10
1
0.1
0.01
0.001
B
Pearson
Pleiotropy
-1
0
1
Spores 1
L-GA 0.3 1
L-GG 0.6 0.6 1
L-P -0 0.3 0.3 1
P-GG 0.2 0.6 0.7 0.3 1
P-P -0 0.5 0.3 0.6 0.7 1
L-AP -0.2 0 -0.3 0.1 -0.1 -0.1 1
L-A -0.1 0 0.2 0.4 0.4 0.4 0.1 1
P-A -0.5 -0.1 -0.3 0.2 -0.1 0.1 0.2 0.6 1
Spores L-GA L-GG L-P P-GG P-P L-AP L-A P-A
C
X2 = 105.3 (p-value = <0.0001)
X2 = 60.8 (p-value = <0.0001)
X2 = 48.6 (p-value = <0.0001)
2%
32%
36%
70%
Percentage
100
80
60
40
20
0
Pleiotropy
Control Liquid
(1 condition)
Liquid
(5 conditions)
Liquid & Pellicles
(8 conditions)
Liquid, Pellicles & Spores
(9 conditions)

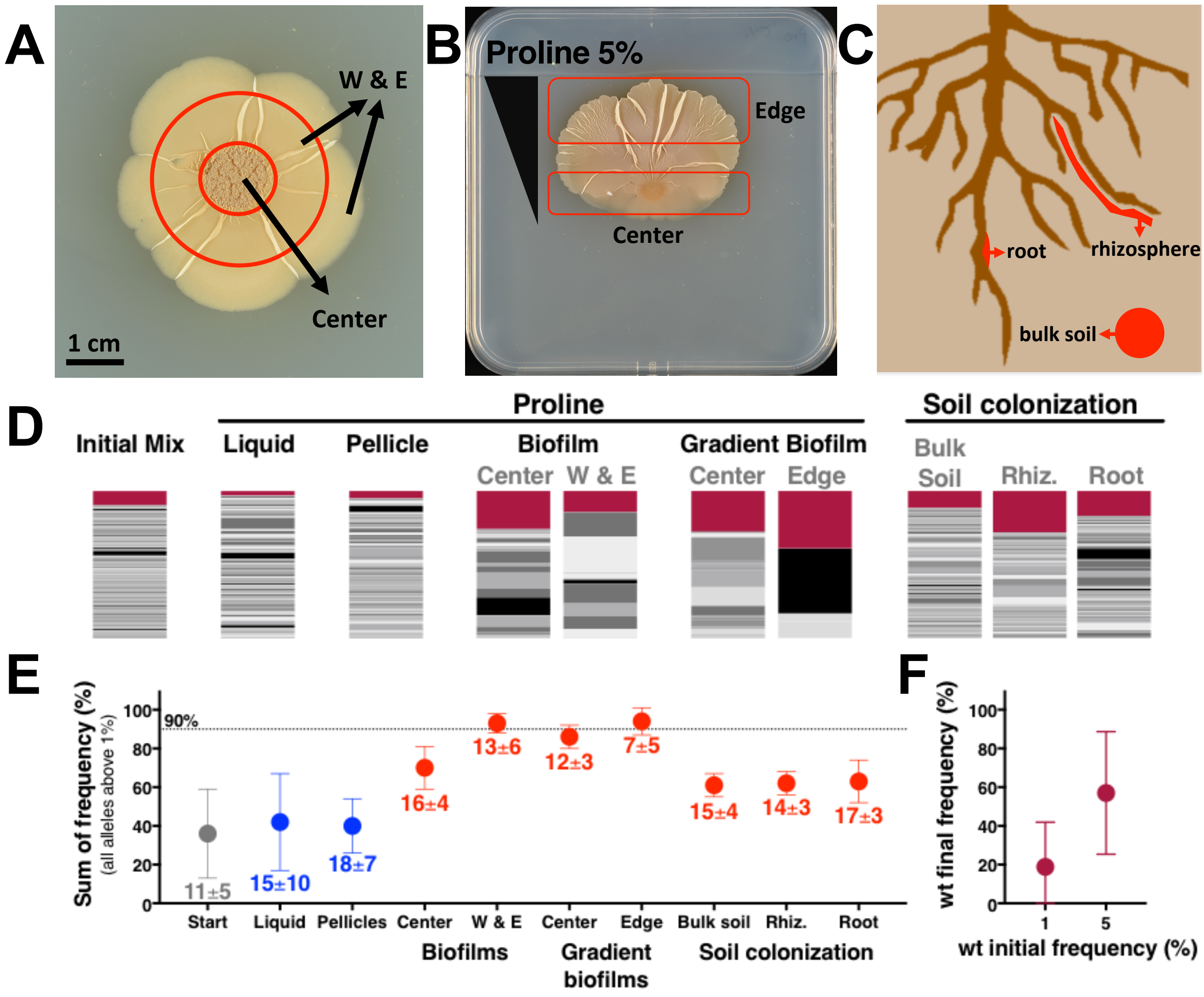
A
W & E
Center
1 cm
B
Proline 5%
Edge
Center
C
root
rhizosphere
bulk soil
D
Proline
Soil colonization
Initial Mix
Liquid
Pellicle
Biofilm
Center
W & E
Gradient Biofilm
Center
Edge
Bulk Soil
Rhiz.
Root
E
Sum of frequency (%)
(all alleles above 1%)
90%
11±5
15±10
18±7
16±4
13±6
12±3
7±5
15±4
14±3
17±3
Start
Liquid
Pellicles
Center
W & E
Center
Edge
Bulk soil
Rhiz.
Root
Biofilms
Gradient biofilms
Soil colonization
F
wt final frequency (%)
wt initial frequency (%)

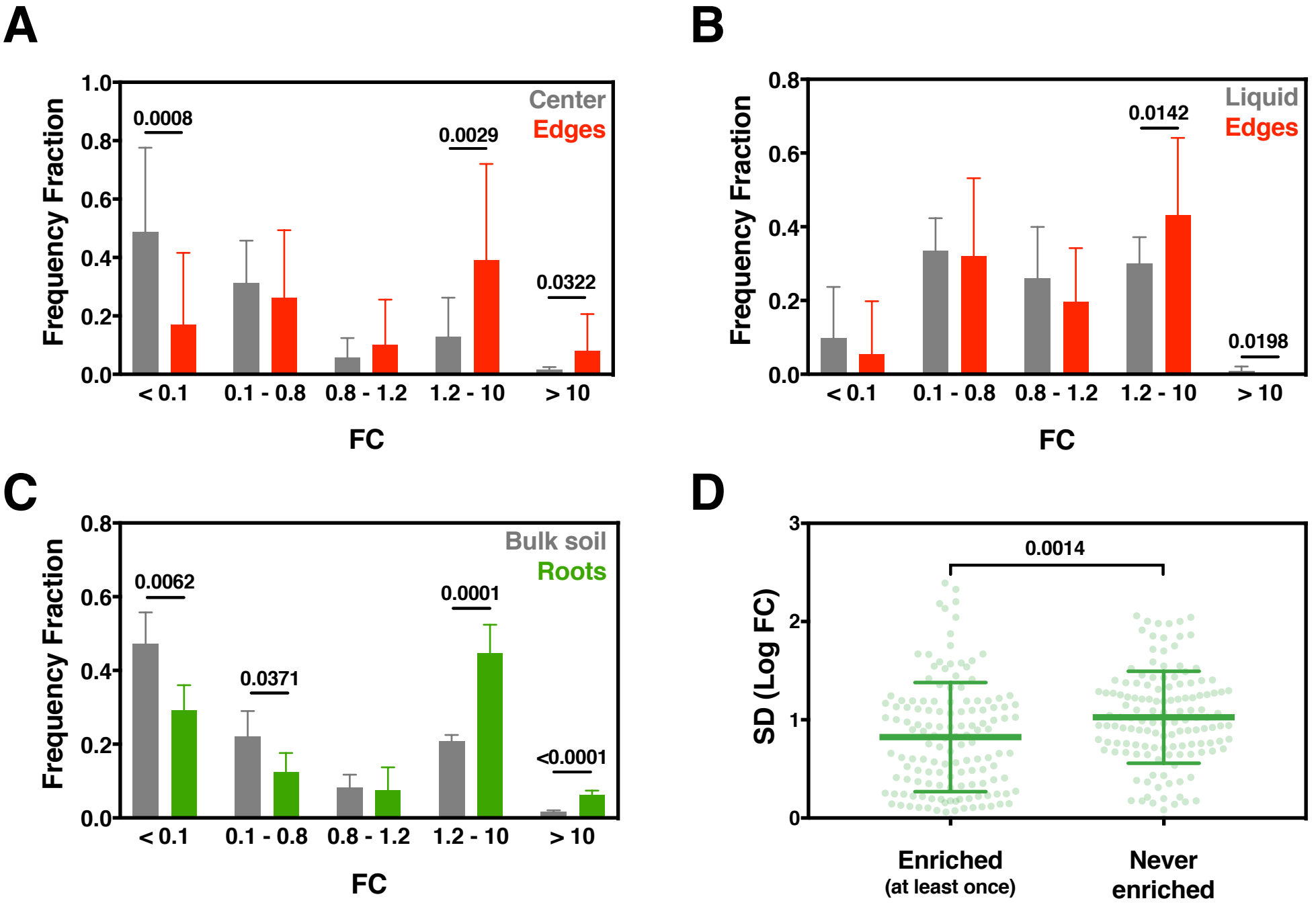
A
Frequency Fraction
1.0
0.8
0.6
0.4
0.2
0.0
Center
Edges
0.0008
0.0029
0.0322
< 0.1
0.1 - 0.8
0.8 - 1.2
1.2 - 10
> 10
FC
B
Frequency Fraction
0.8
0.6
0.4
0.2
0.0
Liquid
Edges
0.0142
0.0198
< 0.1
0.1 - 0.8
0.8 - 1.2
1.2 - 10
> 10
FC
C
Frequency Fraction
0.8
0.6
0.4
0.2
0.0
Bulk soil
Roots
0.0062
0.0371
0.0001
<0.0001
< 0.1
0.1 - 0.8
0.8 - 1.2
1.2 - 10
> 10
FC
D
SD (Log FC)
3
2
1
0
0.0014
Enriched
(at least once)
Never
enriched

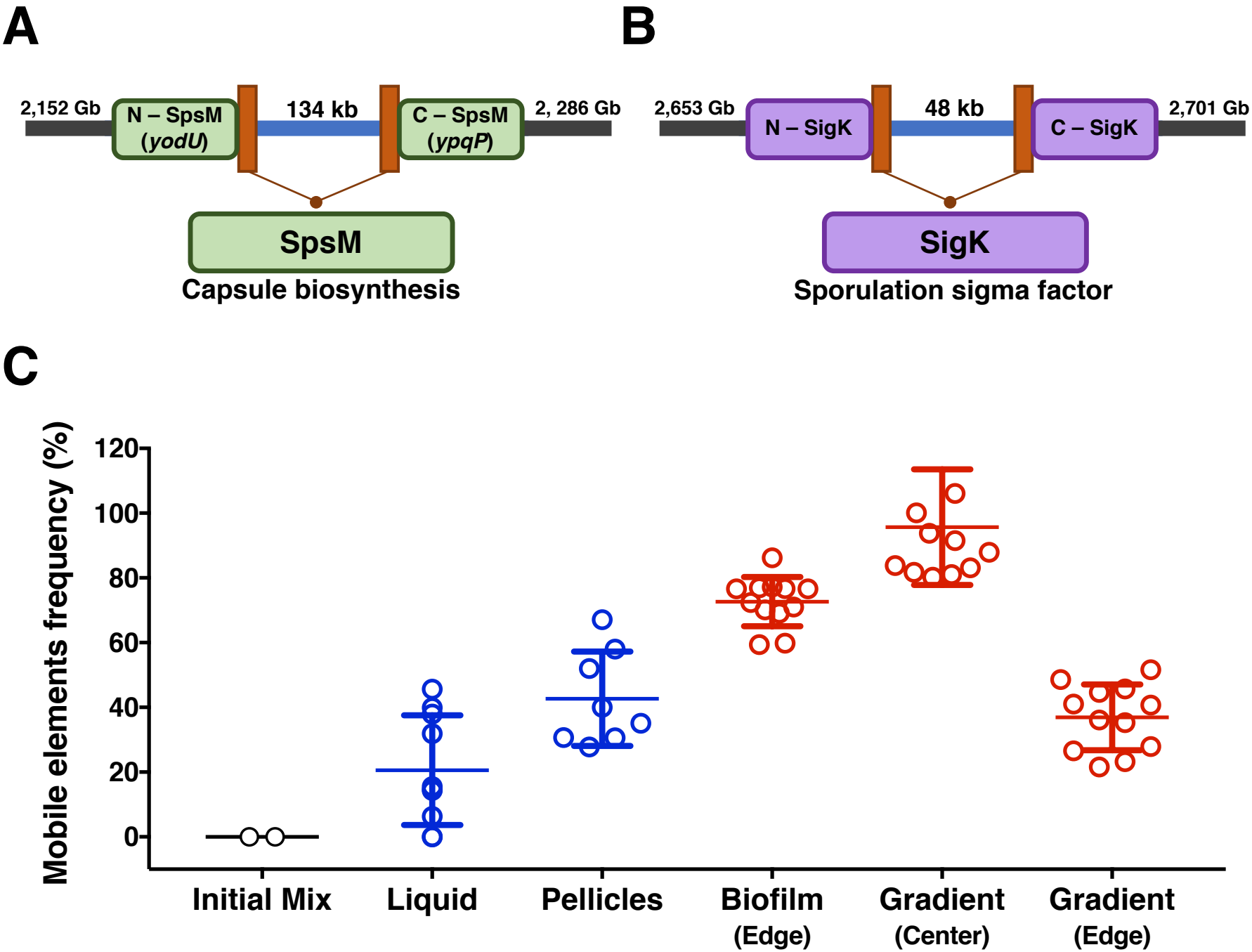
A
2,152 Gb
N – SpsM
(yodU)
134 kb
C – SpsM
(ypqP)
2, 286 Gb
SpsM
Capsule biosynthesis
B
2,653 Gb
N – SigK
48 kb
C – SigK
2,701 Gb
SigK
Sporulation sigma factor
C
Mobile elements frequency (%)
120
100
80
60
40
20
0
Initial Mix
Liquid
Pellicles
Biofilm
(Edge)
Gradient
(Center)
Gradient
(Edge)

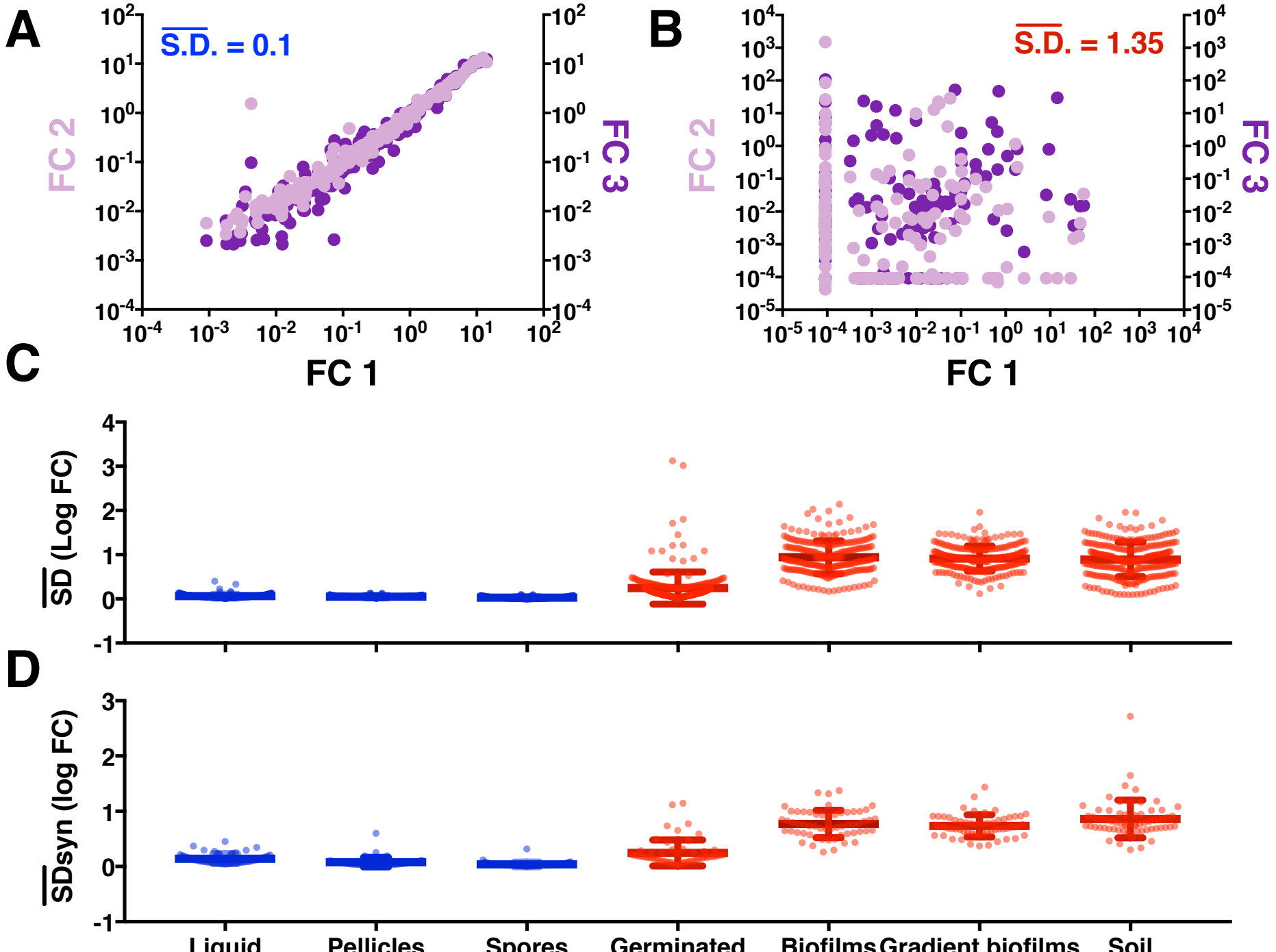
A
S.D. = 0.1
FC 2
FC 3
FC 1
B
S.D. = 1.35
FC 2
FC 3
FC 1
C
SD (Log FC)
D
SDsyn (log FC)
Liquid
Pellicles
Spores
Germinated
Biofilms
Gradient biofilms
Soil